THE JOURNAL OF PHYSICAL CHEMISTRY Letters

pubs.acs.org/JPCL

Dynamics of Ion Assembly in Solution: 2DIR Spectroscopy Study of LiNCS in Benzonitrile

Minbiao Ji,[†,‡] Sungnam Park,[§] and Kelly J. Gaffney*[,†]

[†]PULSE Institute for Ultrafast Energy Science, SLAC National Accelerator Laboratory, Stanford University, Stanford, California 94305, [‡]Department of Physics, Stanford University, Stanford, California 94305, and [§]Department of Chemistry, Korea University, Seoul, South Korea

ABSTRACT The solute−solvent interaction dictates the equilibrium structure of ionic assemblies in solution, ranging from free ions, ion pairs, ion-pair dimers, and ion-pair tetramers to nanoparticles and ionic crystals. We use two-dimensional infrared (2DIR) spectroscopic measurements of the antisymmetric CN stretch of thiocyanate (NCS^-) to study the equilibrium chemical exchange between the spectrally distinct ion pair and the ion-pair dimer in benzonitrile. We observe this chemical exchange to occur with a 36 ± 4 ps time constant. Our measurement indicates that 2DIR will provide a useful tool for investigating the dynamics of ion assembly in solution.

SECTION Kinetics, Spectroscopy

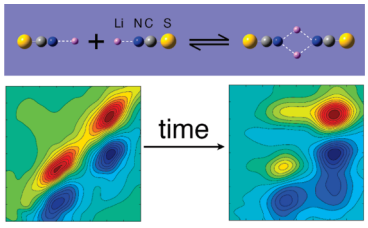

The solvent-mediated interaction of ions has wide-ranging impact in chemistry, biology, and materials science.[1−6] The solvation of ions influences ion mobility, the folding of proteins, ionic assembly, and crystal nucleation. Understanding the physicochemical phenomena that determine the mobility of lithium cations in aprotic solvents has particular technological significance due to the importance of lithium salt electrolytes in secondary lithium ion batteries.[7] The conductivity of lithium solutions has been the main focus of the research on these ionic solutions,[8−11] but the molecular-scale events that dictate the dynamics of ion transport remain poorly understood. Ionic assembly will reduce the conductivity of the ionic solutions by reducing charge carrier densities through the formation of neutral charge aggregates, such as ion pairs, ion-pair dimers, and higher-order aggregates.[12] Understanding the dynamics of these aggregates, as well as the dynamics of their formation and dissociation, will help us understand how solute−solvent interactions control the properties of electrolytes.

Lithium salts form several types of ionic assemblies in solution depending on the properties of the solvent. Lithium thiocyanate (LiNCS) has proven to be an excellent salt to investigate the impact of solvation on ionic assembly, particularly with vibrational spectroscopy. IR and Raman spectroscopy have revealed Li^+−anion pairing and aggregation in many solutions[13−21] based on the charge-aggregate-dependent shifts in anion vibrational modes. For LiNCS, the strong antisymmetric CN stretch (υ_{CN}) is widely used to determine the structure and propensity of different ionic assemblies in solution.[14,15,18,20,21] LiNCS dissolved in benzonitrile solution shows two main υ_{CN} peaks in the IR absorption spectrum, which have been assigned to the ion pair, LiNCS, and the ion-pair dimer, $(LiNCS)_2$.[20] These structures coexist in equilibrium, with the ion pair absorbing at higher frequency than the ion-pair dimer. The spectral distinction between the υ_{CN} vibration in these ionic configurations provides the opportunity to investigate the chemical exchange between the ionic assemblies with multidimensional vibrational correlation (2DIR) spectroscopy.

2DIR spectroscopy provides a robust experimental tool to study equilibrium chemical exchange occurring on the picosecond time scale.[22−29] We have used 2DIR spectroscopy to investigate the exchange dynamics of the LiNCS pair dimer system. Detailed numerical analysis of the time-dependent 2D spectra shows that ion-pair dimers dissociate to form ion pairs with a 60 ± 5 ps time constant in a 1.2 M solution of LiNCS in benzonitrile. The ion pair association occurs with a 90 ± 7 ps time constant. Our measurement demonstrates that 2DIR studies can be extended to a new class of chemical reaction.

The ionic association of Li^+ and NCS^- in aprotic solvents leads to a multitude of ionic assemblies depending on the specific properties of the solvent and the ionic concentration.[15,18,30,31] In strong polar solvents, such as dimethyl sulfoxide and acetonitrile, LiNCS exists predominantly as free ions at low ionic concentration and ion pairs at high concentration. In normal ethers, such as diethyl and dibutyl ether, LiNCS forms ion-pair dimers $(LiNCS)_2$, while in isopropyl ethyl ether and triethylamine, LiNCS mainly forms ion-pair tetramers $(LiNCS)_4$.[18] Figure 1 shows the concentration-dependent FTIR spectra of the υ_{CN} of NCS^-. The peak at 2073 cm^{-1} corresponds to the υ_{CN} absorption of the ion pair, while the peak at 2042 cm^{-1} corresponds to the υ_{CN} absorption of the ion pair dimer. For the 0.1 M LiNCS spectrum, the ion pair absorption dominates. With increasing LiNCS concentration, the ion-pair dimer absorption intensity grows. At 1.2 M LiNCS, the ion pair

Received Date: April 15, 2010
Accepted Date: May 14, 2010
Published on Web Date: May 24, 2010

DOI: 10.1021/jz100486x | *J. Phys. Chem. Lett.* **2010**, *1*, 1771–1775

and ion-pair dimer peaks have comparable amplitude. The determination of the absorption cross section and concentrations of the ion pair and ion-pair dimer will be discussed in conjunction with the kinetic model. Raman, FTIR, and NMR studies confirm that the ion-pair dimer has a quadrupole charge distribution.[16,31] The small blue-shifted shoulder at roughly 2100 cm^{-1} has been assigned to a chain aggregate. We use the 1.2 M solution in this study and focus on the pair dimer equilibrium chemical exchange dynamics using 2DIR spectroscopy.

Two-dimensional infrared (2DIR) spectroscopy monitors thermal equilibrium dynamics occurring on the picosecond time scale by vibrationally labeling molecules with their initial frequencies (ω_τ) and then recording the final frequencies (ω_m) of the initially labeled molecules after an experimentally controlled waiting time (T_w).[23−26,28,32−34] This spectroscopic technique can observe chemical exchange events as slow as a few times the vibrational lifetime and as fast as $1/\Delta\omega$, where $\Delta\omega$ equals the vibrational frequency difference between the interconverting species. 2DIR spectra, $S(\omega_\tau,\omega_m,T_w)$, are displayed by correlating the initial frequency (ω_τ) and final frequency (ω_m) as a function of waiting times (T_w). The well-separated υ_{CN} absorption of NCS^- in the LiNCS ion pair and that in the $(LiNCS)_2$ ion-pair dimer make the chemical exchange between these distinct ionic configurations an excellent candidate for investigation with 2DIR spectroscopy.

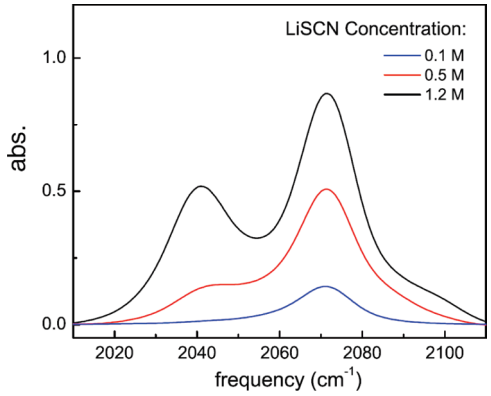

Figure 1. Concentration-dependent FTIR spectra of a LiNCS/benzonitrile solution. While LiNCS appears mainly as ion pairs absorbing at 2073 cm^{-1} at low ionic concentration, it forms ion-pair dimers at higher concentration, contributing a new absorption peak at 2042 cm^{-1}.

Figure 2A shows experimental 2DIR spectra for the LiNCS pair dimer system at different T_w. The spectra have multiple peaks representing various vibrational transitions. The red peaks along the diagonal ($\omega_\tau = \omega_m$) correspond to the fundamental transitions ($\upsilon = 0 \rightarrow 1$) for each distinct ionic configuration. The blue peaks, with ω_m red-shifted from the diagonal peaks by the vibrational anharmonicity, correspond to the excited-state transitions ($\upsilon = 1 \rightarrow 2$) for the distinct ionic configurations.

The T_w-dependent spectra contain rich dynamical information about the solute−solvent interaction. Here, we focus on the chemical dynamics of ion-pair dimer formation and dissociation that can be accessed by measuring the T_w-dependent cross-peak intensities of the 2DIR spectra. The T_w-dependent change of the peak shapes that result from spectral diffusion will be addressed in a future publication. The peaks at (ω_τ, ω_m) equal to (2073 cm^{-1}, 2073 cm^{-1}) and (2073 cm^{-1}, 2050 cm^{-1}) represent the $\upsilon = 0 \rightarrow 1$ and $1 \rightarrow 2$ vibrational transitions of the LiNCS ion pair, and the peaks at (2042 cm^{-1}, 2042 cm^{-1}) and (2042 cm^{-1}, 2022 cm^{-1}) represent the $\upsilon = 0 \rightarrow 1$ and $1 \rightarrow 2$ vibrational transitions of the $(LiNCS)_2$ ion-pair dimer. The cross-peak at (2042 cm^{-1}, 2073 cm^{-1}) results from the ion-pair dimer dissociation to two ion pairs, and the cross-peak at (2073 cm^{-1}, 2022 cm^{-1}) results from the association of two ion pairs to form an ion-pair dimer, detected with the $\upsilon = 1 \rightarrow 2$ transition of the ion-pair dimer. The two additional cross-peaks that exist at (2042 cm^{-1}, 2050 cm^{-1}) and (2073 cm^{-1}, 2042 cm^{-1}) cannot be resolved in Figure 2A. This occurs because these peaks overlap with the stronger $\upsilon = 0 \rightarrow 1$ absorption of the ion-pair dimer and the $\upsilon = 1 \rightarrow 2$ absorption of the ion pair.

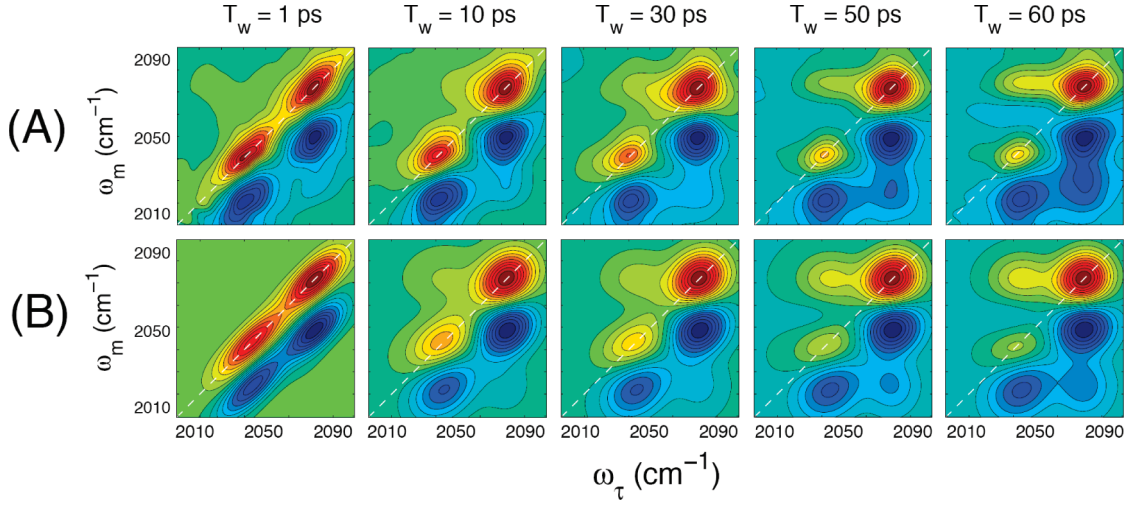

Figure 2. T_w-dependent 2DIR spectra of the LiNCS pair dimer equilibrium. Experimental results are shown in (A), with the growth in the cross peak intensity as a function of T_w providing the clear signature of pair dimer conformational exchange. Numerically calculated spectra are shown in (B), with an exchange time constant of $\tau_{ex} = 36 \pm 4$ ps.

DOI: 10.1021/jz100486x | J. Phys. Chem. Lett. 2010, 1, 1771–1775

The simulation shown in Figure 2B does account for these peaks, and they must be included in the model to achieve agreement between the simulation and the experiment.

For T_w values much larger than the excited-state lifetime, the 2DIR spectra showns a signal that results from vibrational-relaxation-induced heating of the solution. We have limited our analysis to $T_w \leq 60$ to ensure that this heating effect does not impact our data analysis. For a 60 ps waiting time, the cross-peak intensity exceeds the magnitude of the thermal contribution by more than a factor of 5. We discuss the dynamics of this thermalization in detail in the Supporting Information.

We numerically calculated the linear IR spectrum and the T_w-dependent 2DIR spectra using a response function formalism based on diagrammatic perturbation theory with input parameters estimated from the linear and nonlinear experimental results.[35] A detailed description of the two-species exchange kinetic model used in the response function calculation of T_w-dependent 2D spectra can be found in the work of Kwak et al.[36] As indicated below, the same model can be used to treat the ion pair dimer system.

The chemical equation for the ion pair and dimer equals

$$2\mathrm{P} \underset{k_{\mathrm{D-P}}}{\overset{k_{\mathrm{P-D}}}{\rightleftharpoons}} \mathrm{D} \qquad (1)$$

with P representing the ion pair and D representing the ion-pair dimer and k_{P-D} and k_{D-P} representing the forward and backward reaction rate constants. Ignoring the activity coefficients of ionic species in solution, the equilibrium constant, K_{eq}, equals

$$K_{eq} = \frac{[\mathrm{D}]_{eq}}{[\mathrm{P}]_{eq}^2} = \frac{k_{\mathrm{P-D}}}{k_{\mathrm{D-P}}} \qquad (2)$$

where $[P]_{eq}$ and $[D]_{eq}$ are the equilibrium concentrations of the LiNCS ion pair and the $(LiNCS)_2$ ion-pair dimer. For 2DIR vibrational studies, vibrational excitation does not shift the chemical equilibrium. Instead, 2DIR monitors the thermal fluctuation-driven chemical exchange of vibrationally labeled molecules.

The second-order kinetics of the dimerization reaction can be simplified to pseudo-first-order kinetics. We redefine $[P]_{eq} = [P]_v + [P]_0$ and $[D]_{eq} = [D]_v + [D]_0$, with $[P]_v$ and $[D]_v$ representing the vibrationally labeled molecules and $[P]_0$ and $[D]_0$ representing the leftover ground-state molecules. Since laser excitation satisfies $[P]_v \ll [P]_0$ and $[D]_v \ll [D]_0$ (we excited ~5% of the ion pair molecules), the probability of two excited ion pairs combining to form a dimer or the probability of both NCS^- ions in one dimer being vibrationally excited is very low. Specifically, $[P]_v = (J_0\sigma_P)[P]_{eq}$ and $[D]_v = (J_0\sigma_D)[D]_{eq}$, where J_0 is the photon fluence, and σ_i is the absorption cross section of species i, $J_0\sigma_i$ is the average number of photons absorbed per molecule of species i.[37] For the low excitation limit, $J_0\sigma \ll 1$, we can rewrite the equilibrium equation of the excited molecule subensemble to be

$$\mathrm{P}_v + \mathrm{P}_0 \rightleftharpoons \mathrm{D}_v \qquad (3)$$

This can be reduced to the standard two-species exchange kinetic model,[28,36] with an effective equilibrium constant for the subensemble equal to $K_v^{eff} = ([D]_v/[P]_v) = (k_{P-D}^{eff}/k_{D-P}) = (\sigma_D/\sigma_P)K_{eq}[P]_{eq}$ and an effective forward reaction rate constant of $k_{P-D}^{eff} = (\sigma_D/\sigma_P)k_{P-D}[P]_{eq}$. Since 2DIR spectroscopy only accesses the dynamics of the excited species, P_v and D_v, we only directly measure k_{D-P} and k_{P-D}^{eff}.

These effective first-order kinetics allow us to use the analytical solution to the exchange kinetic model[28,36] developed by Kwak et al. in our response function calculations. The parameters involved in the calculation are the center frequencies ω_0, anharmonicities $\Delta\omega$, population lifetimes T_1, orientation relaxation lifetimes τ_{or}, exchange rate, equilibrium concentrations, transition dipole moments μ_{01}, and frequency−frequency correlation functions. The population and orientational relaxation rate have been measured with polarization-resolved IR pump−probe measurements, and the results can be found in the Supporting Information. Joint fitting of the FTIR and 2DIR spectrum for $T_w = 0.2$ ps allows us to fit the transition dipole moments and concentrations for the ion pair and ion-pair dimer since each spectrum depends linearly on the concentration, while the FTIR spectral amplitude is proportional to μ_{01}^2 and the 2DIR spectral amplitude is proportional to μ_{01}^4. The frequency−frequency correlation functions influence the vibrational line shapes in the 2DIR spectra but do not influence the peak volumes. This makes the extraction of chemical exchange dynamics insensitive to the details of the line shape analysis, particularly when using peak volumes to determine the exchange dynamics. The best fit of the key parameters for the exchange dynamics are shown in Table 1. The extraction of the spectral diffusion dynamics from the T_w-dependent line shapes will be addressed in a later publication.

Figure 3 shows the fit of the experimental peak volumes for the diagonal and cross-peaks, and Figure 2B shows the fit of the 2DIR spectra with the response function calculations.

Table 1. Parameters Used to Numerically Calculate FTIR Spectrum and T_w-Dependent 2DIR Spectra

	T_1(ps)	τ_{or}(ps)	ω_0(cm^{-1})	$\Delta\omega$(cm^{-1})	μ_{01}	conc.
pair	21.4	75	2071	23	1	1
dimer	19.5	81	2042	20	1.42	0.38

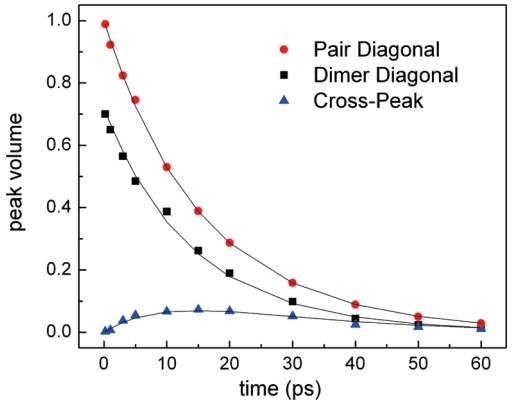

Figure 3. T_w-dependent peak volumes of the ion pair and ion pair dimer diagonal signals and the cross-peak extracted from the 2D spectra in Figure 2A. Kinetic model analysis provides an ion pair dimer conformational exchange time constant of $\tau_{ex} = 36 \pm 4$ ps.

DOI: 10.1021/jz100486x | J. Phys. Chem. Lett. 2010, 1, 1771–1775

We extract an ion pair association time constant of $(k_{P-D}^{eff})^{-1} = 90 \pm 7$ ps, an ion-pair dimer dissociation time constant of $k_{D-P}^{-1} = 60 \pm 5$ ps, and a total exchange time of $\tau_{ex} = (k_{P-D}^{eff} + k)_{D-P}^{-1} = 36 \pm 4$ ps from these calculations.

Our measurement clearly shows the accessibility of ion assembly dynamics in aprotic solvents to 2DIR spectroscopy. Although this study focuses on the ion pair dimer equilibrium in the LiNCS−benzonitrile solution, LiNCS salt appears to provide an excellent system for investigating how solvents control the dynamics of ion assembly. Preliminary measurements in other solvents indicate that we will be able to observe the exchange dynamics of thiocyanate extending from the free anion to the ion-pair tetramer. By correlating these chemical exchange dynamics with configuration-dependent solvation and orientational relaxation dynamics, we intend to gain a molecular-scale understanding of the dynamics of electrolyte solutions and how these dynamics influence ion assembly and transport in solution.

EXPERIMENTAL SECTION

A detailed description of the 2DIR experimental methodology can be found in previous publications.[28,33] We purchased benzonitrile (99.9%) and LiNCS hydrate from Sigma−Aldrich. We used benzonitrile as received, and dried the $LiSCN \cdot xH_2O$ with a literature procedure.[20] We prepared the solution by dissolving LiNCS in benzonitrile and then centrifuging the solution for 15 min to precipitate the suspensed particles. We sealed the sample between two CaF_2 widows spaced by a 3 μm PET spacer to generate a maximum absorbance of roughly 0.4 for the 1.2 M LiNCS solution. We performed the vibrational measurements at 22 °C over a spectral range from 1984 to 2110 cm^{-1} with a resolution of 4 cm^{-1}.

SUPPORTING INFORMATION AVAILABLE Polarization-selective pump−probe spectroscopy and thermal contribution to 2DIR spectra. This material is available free of charge via the Internet at http://pubs.acs.org.

AUTHOR INFORMATION

Corresponding Author:

*To whom correspondence should be addressed. Email: kgaffney@slac.stanford.edu.

ACKNOWLEDGMENT This research is supported through the PULSE Institute at SLAC National Accelerator Laboratory by the U.S. Department of Energy, Office of Basic Energy Sciences. S.P. and K.G. acknowledge additional support from the W. M. Keck Foundation. S.P. thanks Prof. Minhaeng Cho for helpful discussion and Korea University for a new faculty grant.

REFERENCES

(1) Baldwin, R. L. How Hofmeister Ion Interactions Affect Protein Stability. *Biophys. J.* **1996,** *71*, 2056–2063.

(2) Kuhn, T.; Schwalbe, H. Monitoring the Kinetics of Ion-Dependent Protein Folding by Time-Resolved NMR Spectroscopy at Atomic Resolution. *J. Am. Chem. Soc.* **2000,** *122*, 6169–6174.

(3) Otzen, D. E.; Oliveberg, M. Salt-Induced Detour through Compact Regions of the Protein Folding Landscape. *Proc. Natl. Acad. Sci. U.S.A.* **1999,** *96*, 11746–11751.

(4) Castleman, A. W.; Holland, P. M.; Keesee, R. G. The Properties of Ion Clusters and Their Relationship to Heteromolecular Nucleation. *J. Chem. Phys.* **1978,** *68*, 1760.

(5) Onsager, J. H. a. L. Dielectric Dispersion and Dielectric Friction in Electrolyte Solutions. I. *J. Chem. Phys.* **1977,** *67*, 4850.

(6) Faul, C. F. J.; Antonietti, M. Ionic Self-Assembly: Facile Synthesis of Supramolecular Materials. *Adv. Mater.* **2003,** *15*, 673–683.

(7) Xu, K. Nonaqueous Liquid Electrolytes for Lithium-Based Rechargeable Batteries. *Chem. Rev.* **2004,** *104*, 4303–4417.

(8) Ding, M. S.; Xu, K.; Zhang, S. S.; Amine, K.; Henriksen, G. L.; Jow, T. R. Change of Conductivity with Salt Content, Solvent Composition, and Temperature for Electrolytes of LiPF6 in Ethylene Carbonate−Ethyl Methyl Carbonate. *J. Electrochem. Soc.* **2001,** *148*, A1196–A1204.

(9) Michael, S. D.; Jow, T. R. Conductivity and Viscosity of PC-DEC and PC-EC Solutions of LiPF6. *J. Electrochem. Soc.* **2003,** *150*, A620–A628.

(10) Xiao, L. F.; Cao, Y. L.; Ai, X. P.; Yang, H. X. Optimization of EC-based Multisolvent Electrolytes for Low Temperature Applications of Lithium-Ion Batteries. *Electrochim. Acta* **2004,** *49*, 4857–4863.

(11) Kazuishi, M.; Keiichiro, A. Ionic Conduction in LiSCN/Dimethylformamide/Poly(propylene oxide) System II. Mobility of Lithium and Thiocyanate Ions. *J. Polym. Sci., Part B: Polym. Phys.* **1995,** *33*, 947–954.

(12) Nicolas, M.; Reich, R. Ionic Association of Lithium Perchlorate in Low Dielectric Constant Media from Very Dilute Solutions to Saturation at 293 and 198 K. *J. Chem. Phys.* **2002,** *83*, 749–756.

(13) Schantz, S.; Sandahl, J.; Borjesson, L.; Torell, L. M.; Stevens, J. R. Ion Pairing in Polymer Electrolytes — A Comparative Raman-Study of $NaCF_3SO_3$ Complexed in Poly(Propylene-Glycol) and Dissolved in Acetonitrile. *Solid State Ionics* **1988,** *28*, 1047–1053.

(14) Chabanel, M.; Menard, C.; Guiheneu, G Infrared Spectrum of Lithium Thiocyanate in Solution — Association of Ions in Aggregate and Pair Form. *Acad. Sci. Paris, Ser. C* **1971,** *272*, 253.

(15) Chabanel, M.; Wang, Z. Vibrational Study of Ionic Association in Aprotic-Solvents. 6. Dimerization of Lithium, Soldium and Potassium Isothiocyanate ion pairs in Tetrahydrofuran and in 1,3-Dioxolane. *J. Phys. Chem.* **1984,** *88*, 1441–1445.

(16) Paoli, D.; Lucon, M.; Chabanel, M. Vibrational Study of Ionic Association in Aprotic-Solvents. 2. Structure And Force Constants of the Lithium Thiocyanate Dimer in Ether Solutions. *Spectrochim. Acta, Part A* **1979,** *35*, 593–596.

(17) Rannou, J.; Chabanel, M. Vibrational Study of Ionic Association in Aprotic-Solvents. 3. Thermodynamics of ion pairing in Alkali Cyanate−Dimethyl Sulfoxyde Solutions. *J. Chim. Phys. Phys. Chim. Biol.* **1980,** *77*, 201–204.

(18) Chabanel, M.; Lucon, M.; Paoli, D. Vibrational Study of Ionic Association in Aprotic-Solvents. 5. Formation and Structure of the Lithium Isothiocyanate Tetramer in Alkyl Ethers and in Tertiary-Amines. *J. Phys. Chem.* **1981,** *85*, 1058–1061.

(19) Burba, C. M.; Frech, R. Spectroscopic Measurements of Ionic Association in Solutions of LiPF6. *J. Phys. Chem. B* **2005,** *109*, 15161–15164.

(20) Barthel, J.; Buchner, R.; Wismeth, E. FTIR spectroscopy of ion solvation of $LiClO_4$ and LiSCN in acetonitrile, benzonitrile,

and propylene carbonate. *J. Solution Chem.* **2000,** *29*, 937–954.
(21) Paoli, D.; Lucon, M.; Chabanel, M. Vibrational Study of Ionic Association in Aprotic-Solvents. 1. Ion Pairs of Alkali And Silver Thiocyanate in Dimethylformanide or Dimethylthioformamide. *Spectrochim. Acta, Part A* **1978,** *34*, 1087–1091.
(22) Zheng, J.; Kwak, K.; Xie, J.; Fayer, M. D. Ultrafast Carbon–Carbon Single-Bond Rotational Isomerization in Room-Temperature Solution. *Science* **2006,** *313*, 1951–1955.
(23) Zheng, J.; Kwak, K.; Asbury, J.; Chen, X.; Piletic, I. R.; Fayer, M. D. Ultrafast Dynamics of Solute–Solvent Complexation Observed at Thermal Equilibrium in Real Time. *Science* **2005,** *309*, 1338–1343.
(24) Cahoon, J. F.; Sawyer, K. R.; Schlegel, J. P.; Harris, C. B. Determining Transition-State Geometries in Liquids Using 2D-IR. *Science* **2008,** *319*, 1820–1823.
(25) Woutersen, S.; Mu, Y.; Stock, G.; Hamm, P. Hydrogen-Bond Lifetime Measured by Time-Resolved 2D-IR Spectroscopy: N-Methylacetamide in Methanol. *Chem. Phys.* **2001,** *266*, 137–147.
(26) Kim, Y. S.; Hochstrasser, R. M. Chemical Exchange 2D IR of Hydrogen-Bond Making and Breaking. *Proc. Natl. Acad. Sci. U. S.A.* **2005,** *102*, 11185–11190.
(27) Moilanen, D. E.; Wong, D.; Rosenfeld, D. E.; Fenn, E. E.; Fayer, M. D. Ion–Water Hydrogen-Bond Switching Observed with 2D IR Vibrational Echo Chemical Exchange Spectroscopy. *Proc. Natl. Acad. Sci. U.S.A.* **2009,** *106*, 375–380.
(28) Park, S.; Odelius, M.; Gaffney, K. J. Ultrafast Dynamics of Hydrogen Hond Exchange In Aqueous Ionic Solutions. *J. Phys. Chem. B* **2009,** *113*, 7825–7835.
(29) Park, S.; Ji, M.; Gaffney, K. J. Ligand Exchange Dynamics in Aqueous Solution Studied with 2DIR Spectroscopy. *J. Phys. Chem. B* **2010,** *114*, 6693–6702.
(30) Goralski, P.; Chabanel, M. Vibrational Study of Ionic Association in Aprotic-Solvents. 11. Formation And Structure of Mixed Aggregates Between Lithium Halides And Lithium Thiocyanate. *Inorg. Chem.* **1987,** *26*, 2169–2171.
(31) Vaes, J.; Chabanel, M.; Martin, M. L. Ionic Interactions in Lithium Thiocyanate Solutions. Nitrogen-15 and Lithium-7 Nuclear Magnetic Resonance Studies. *J. Chem. Phys.* **2002,** *82*, 2420–2423.
(32) Park, S.; Fayer, M. D. Hydrogen Bond Dynamics in Aqueous Nabr Solutions. *Proc. Natl. Acad. Sci. U.S.A.* **2007,** *104*, 16731–16738.
(33) Park, S.; Kwak, K.; Fayer, M. D. Ultrafast 2D-IR Vibrational Echo Spectroscopy: A Probeof Molecular Dynamics. *Laser Phys. Lett.* **2007,** *4*, 704–718.
(34) Park, S.; Moilanen, D. E.; Fayer, M. D. Water Dynamics: The Effects of Ions and Nanoconfinement. *J. Phys. Chem. B* **2008,** *112*, 5279–5290.
(35) Khalil, M.; Demirdoven, N.; Tokmakoff, A. Coherent 2D IR Spectroscopy: Molecular Structure and Dynamics in Solution. *J. Phys. Chem. A* **2003,** *107*, 5258–5279.
(36) Kwak, K.; Zheng, J.; Cang, H.; Fayer, M. D. Ultrafast Two-Dimensional Infrared Vibrational Echo Chemical Exchange Experiments and Theory. *J. Phys. Chem. B* **2006,** *110*, 19998–20013.
(37) Ji, M. B.; Park, S.; Connor, S. T.; Mokari, T.; Cui, Y.; Gaffney, K. J. Efficient Multiple Exciton Generation Observed in Colloidal PbSe Quantum Dots with Temporally and Spectrally Resolved Intraband Excitation. *Nano Lett.* **2009,** *9*, 1217–1222.

DOI: 10.1021/jz100486x | *J. Phys. Chem. Lett.* **2010,** *1*, 1771–1775